

An average-bond-energy method used for band-offset calculation for a strained heterojunction

This article has been downloaded from IOPscience. Please scroll down to see the full text article.

2000 J. Phys.: Condens. Matter 12 7759

(<http://iopscience.iop.org/0953-8984/12/35/311>)

View [the table of contents for this issue](#), or go to the [journal homepage](#) for more

Download details:

IP Address: 171.66.16.221

The article was downloaded on 16/05/2010 at 06:44

Please note that [terms and conditions apply](#).

An average-bond-energy method used for band-offset calculation for a strained heterojunction

Shu-Ping Li[†], Ren-Zhi Wang^{†‡}, Yong-Mei Zheng^{†‡}, Shu-Hui Cai[†] and Guo-Min He[†]

[‡] CCAST (World Laboratory), PO Box 8730, Beijing 100080, People's Republic of China

[†] Physics Department, Xiamen University, Xiamen, Fujian 361005, People's Republic of China

Received 8 March 2000, in final form 22 June 2000

Abstract. We have extended the average-bond-energy method to study the strained-heterojunction band offset. Through a detailed study of the effect of hydrostatic and uniaxial strains on the energy of the average valence band edge $E_{v,av}$ relative to the average bond energy, we find that $E_{v,av}$ remains basically unchanged under different strain conditions, and that the deformation potential $a_{v,av}$ corresponding to $E_{v,av}$ is much smaller than the a_v for other analogous methods. Thus, in the average-bond-energy method, the valence band offset ΔE_v can be obtained neglecting $a_{v,av}$. It is only necessary to calculate the valence band maximum energy relative to the average bond energy before the strain and to use the experimental values of the deformation potential b and spin-orbit splitting Δ_0 to determine the splitting value for the valence band. It is not necessary to calculate the band structures under various strain conditions. This simplified calculation method involves only a small calculational burden; therefore, it can conveniently be used to predict the strained-heterojunction band offset.

1. Introduction

Semiconductor superlattices and heterostructures are of considerable technological importance because of their unique electronic properties. They allow great flexibility to be achieved in design by the variation of the thickness of the layers and the state of strain. At present, the main method used for designing and tailoring the strained-heterojunction band offset is to adjust the substrate material's lattice constant. This causes the epitaxially grown layer to experience different strain conditions, and thus changes the band structure of the strained-layer and the band offset of the strained heterojunction. The band offset is an important parameter for designing the characteristics of new materials and electronic devices involving heterojunctions and superlattices. Therefore, if the band offset of a strained heterojunction can be conveniently predicted under different conditions of strain, this will undoubtedly be of significance for designing and optimizing new devices. In view of this, Van de Walle and Martin extended the model-solid theory (MST) [1] to include the calculation of strained-heterojunction band offsets [2]. Ohler *et al* [3] recently also adopted a similar method, extending the charge-neutrality-level (CNL) theory founded by Tersoff [4] to include the calculation of the band offsets of strained heterojunctions. In this paper, we review the main features of our average-bond-energy (ABE) [5] method, and suggest a simplified scheme for calculation of the valence band offset (VBO) for strained heterojunctions, through the investigation of the effects of the strain condition on the average valence band edge $E_{v,av}$ relative to the average bond energy E_m . The scheme can considerably reduce the calculational burden and enhance

the reliability of calculation results. It will be more convenient for the calculation of the strained-heterojunction band offsets. In order to allow comparison with the results of Ohler *et al* [3] and Van de Walle [2], most of the material parameters used in this paper are the same as theirs (see table 1).

Table 1. The material parameters used in the calculations of this paper: lattice constants a_0 (in Å), elastic constants C_{11} , C_{12} (in Mbar), spin-orbit splittings Δ_0 (in eV), and the experimental values of the shear deformation potential b (in eV). These values of b are all from reference [3] except that for GaP which is from reference [14].

Semiconductor	a_0	C_{11}	C_{12}	Δ_0	b (experimental)
Si	5.43	16.75	6.5	0.04	-2.10
Ge	5.65	13.15	4.94	0.30	-2.86
InP	5.87	10.22	5.76	0.11	-1.60
InAs	6.06	8.33	4.53	0.38	-1.80
GaP	5.45	14.11	6.26	0.08	-1.50
GaAs	5.65	12.23	5.71	0.34	-1.70
AlAs	5.65	12.50	5.34	0.28	-1.50

In the next section, we present our band-offset calculation method based on the ABE theory. Section 3 contains a description of the effects of strain on band edges. In section 4, we present the numerical testing of the contributions from each strain component. Section 5 contains a description of the simplified ABE method and its application to strain. The last section gives our conclusions.

2. The average-bond-energy method

There are two main groups of methods used in theoretical studies of the heterojunction band offset. One is the methods based on self-consistent supercell calculation (SCSC) or self-consistent interface calculation (SCSI)—for example, the self-consistent supercell calculation of Christensen [6] and the self-consistent interface calculation of Van de Walle and Martin [1]. The linearized augmented-plane-wave (LAPW) method of Zunger and co-workers [7] was the first to determine the difference between the core levels on the two sides of the heterojunction interface by using a self-consistent supercell calculation, and then to calculate the band offset. It is also a method that belongs to this group. In this first group of methods, based on self-consistent calculation, all the effects of an interface are taken into account as a whole. So they are very precise theoretical calculation methods. But the degree of computational complexity of such calculations is very high, and it is difficult to determine what physical mechanisms are dominant in the valence band offset. This group of methods involves a self-consistent supercell calculation for each strain condition; thus the calculational burden will be very large. The other group of methods is based on introducing a certain reference energy level to line up the two bulk band structures of the heterojunction, and then calculating the band offset—for example, the dielectric midgap energy (DME) method [8], the charge-neutrality-point (CNP) method [9], and the tight-binding (TB) method [10]. In this group of methods, because a reference level is adopted to line up the band structures of the heterojunction, it is only necessary to calculate the energy difference between the highest valence level and the reference level to determine the valence band offset of the heterojunction; it is not necessary to perform a self-consistent supercell calculation. Thus the calculational burden is reduced substantially. In the study of the band offset of a strained-layer heterojunction, the deformation potential of the bulk is used to investigate the rules governing the heterojunction band offset and strain conditions.

The average-bond-energy method adopted in this paper also belongs to this second group of methods. The average bond energy and the average-bond-energy method will be briefly introduced below.

Chen and Sher [11] established the method of calculation of the bonding orbital energy E_b and anti-bonding orbital energy E_a for a tetrahedrally bonding semiconductor in a virtual-crystal-approximation study of semiconducting alloy band structure:

$$E_b = \langle b_j(R) | \hat{H} | b_j(R) \rangle = \frac{1}{4N} \sum_{n=1}^4 \sum_k E_n^i(k) \quad (1)$$

$$E_a = \langle a_j(R) | \hat{H} | a_j(R) \rangle = \frac{1}{4N} \sum_{n=5}^8 \sum_k E_n^i(k) \quad (2)$$

where the bonding state is

$$|b_j(R)\rangle = \sum_{n=1}^4 c_{nj} |W_n(R)\rangle$$

and the anti-bonding state is

$$|a_j(R)\rangle = \sum_{n=5}^8 d_{nj} |W_n(R)\rangle$$

($j = 1, 2, 3, 4$ indicates the tetrahedral bonding); the Wannier function can be constructed from the eigenvectors of the energy band:

$$|W_n(R)\rangle = \frac{1}{\sqrt{N}} \sum_k e^{ikR} |\Psi_{nk}\rangle$$

where $E_n^i(k)$ and $|\Psi_{nk}\rangle$ are the eigenvalue and eigenvector of the semiconductor energy band, respectively. Wang *et al* called the mid-point of the energy gap between E_b and E_a the average bond energy:

$$E_m = \frac{1}{2}(E_b + E_a) = \frac{1}{8N} \sum_{n=1}^8 \sum_k E_n^i(k). \quad (3)$$

In a study involving a superlattice LMTO band-structure calculation [12, 13], they found that the average bond energy E_m will be aligned on the two sides of the heterojunction interface. On the basis of this, they established a new reference-level heterojunction band-offset calculation method, taking the average bond energy E_m as the reference level. This method only requires one to calculate the two bulk differences of the (energies of the) highest valence bands E_v from E_m for the heterojunction:

$$E_v = E_v^i - E_m. \quad (4)$$

Then, according to E_m , one aligns the two sides of the heterojunction interface to get the valence band offset of the A/B-type heterojunction:

$$\Delta E_v(A/B) = E_v(B) - E_v(A). \quad (5)$$

Figure 1 also shows how to calculate $\Delta E_v(A/B)$ according to the alignment of the average bond energy.

If material A is the larger-band-gap material of the two materials which constitute the A/B heterojunction, the VBO of the heterojunction is positive. Equation (5) indicates that the heterojunction VBO is determined by the valence band edges relative to E_m . So we should study the rules governing the change of the band edge E_v with different strain conditions

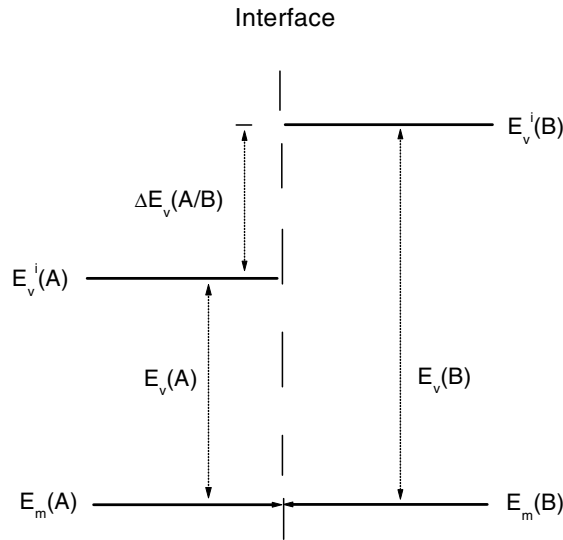


Figure 1. Calculation of $\Delta E_v(A/B)$ based on the average-bond-energy method.

to obtain ΔE_v for the strained heterojunctions. For a strained heterojunction, because the strained-layer band structure changes with the strain conditions, the valence band maximum E_v^i , band edge E_v relative to E_m , and E_m are all related to the strain conditions. We hope to express the relative-energy shift between the average valence band edge and E_m as a function of the hydrostatic pressure and the uniaxial strains, i.e. to find the deformation potential for the average valence band edges relative to E_m . This corresponds to the deformation potential of the band edges relative to the charge-neutrality level or model vacuum level used by the CNL method [3] and the MST method [2].

3. Effects of strain on the valence band edge

If semiconductors A and B have different equilibrium lattice constants a_0 , when A is grown epitaxially on substrate B along the (001) direction, then the epitaxial layer A will be positioned according to the deformation. From elasticity mechanics, one can get for the strained layer A

$$a_{\parallel} = a_{\parallel}^B \quad (6)$$

$$a_{\perp} = a_0 \left[1 - 2 \frac{C_{12}}{C_{11}} (a_{\parallel}/a_0 - 1) \right] \quad (7)$$

where a_{\parallel}^B is the lattice constant of substrate material B in the direction parallel to the interface; a_{\parallel} and a_{\perp} are the lattice constants parallel and perpendicular to the interface, respectively. C_{11} and C_{12} are elastic constants for material A. The biaxial strain is normally divided into isotropic and uniaxial contributions. For the above (001) biaxial strain indicated by equations (6) and (7), the strain tensor components are [2]

$$\varepsilon_{\parallel} = a_{\parallel}/a_0 - 1 \quad \varepsilon_{\perp} = a_{\perp}/a_0 - 1$$

and

$$\text{Tr}(\varepsilon) = 2\varepsilon_{\parallel} + \varepsilon_{\perp} \approx \Omega/\Omega_0 - 1 \quad (8)$$

$$\varepsilon_{ax} = \varepsilon_{\perp} - \varepsilon_{\parallel} = (a_{\perp} - a_{\parallel})/a_0 \quad (9)$$

where Ω_0 and Ω are the unstrained and strained primitive-cell volumes. The trace $\text{Tr}(\varepsilon)$ of the strain tensor is the relative-volume change of the crystal but does not change the symmetry of the crystal, so it mainly induces shifts of the eigenvalues and does not induce the splitting of the degenerate energy band. ε_{ax} is the uniaxial component of the strain tensor; it causes the crystal to deviate from the cubic structure and changes the crystal symmetry but does not change the crystal volume, so it does induce a splitting of the degenerate energy band according to the average values. If the strained heterojunction A/B is grown on substrate material B along the (001) direction, the lattice constant a_{\parallel}^B of substrate material B will remain unchanged, but the parallel lattice constant a_{\parallel} of material A will change and become equal to the value of a_{\parallel}^B (see equation (6)). The uniaxial strain will split the threefold-degenerate valence band into the nondegenerate energy band $E_v^i(1)$ and the doubly degenerate energy band $E_v^i(2)$. The average of $E_v^i(1)$ and $E_v^i(2)$ is $[2E_v^i(2) + E_v^i(1)]/3$; it is called the average of the valence band edges, $E_{v.av}^i$. Let $\delta E_{001} = \frac{2}{3}(E_v^i(1) - E_v^i(2))$; then

$$\delta E_{001} = 2b\varepsilon_{ax} \quad (10)$$

where b is the shear deformation potential. In the above band structure, the spin-orbit splitting has not been included. Because of the effects of the (001) uniaxial strain and spin-orbit splitting, the degenerate valence band will be split into three nondegenerate bands. The energy separations between the three nondegenerate valence band maxima (heavy hole, light hole, and split-off hole) and their average value are given by

$$\Delta E_{v2} = \frac{1}{3}\Delta_0 - \frac{1}{2}\delta E_{001} \quad (11)$$

$$\Delta E_{v1} = -\frac{1}{6}\Delta_0 + \frac{1}{4}\delta E_{001} + \frac{1}{2}\left[\Delta_0^2 + \Delta_0\delta E_{001} + \frac{9}{4}(\delta E_{001})^2\right]^{1/2} \quad (12)$$

$$\Delta E_{v3} = -\frac{1}{6}\Delta_0 + \frac{1}{4}\delta E_{001} - \frac{1}{2}\left[\Delta_0^2 + \Delta_0\delta E_{001} + \frac{9}{4}(\delta E_{001})^2\right]^{1/2} \quad (13)$$

where Δ_0 is the spin-orbit splitting. If the deformation and spin-orbit splitting are considered simultaneously, then $E_v^i = E_{v.av}^i + \Delta E_{vj,max}$, and the valence band maximum with relative to E_m is

$$E_v = E_{v.av} + \Delta E_{vj,max} \quad (14)$$

where $E_{v.av}^i$ is the average valence band maximum which is obtained from a bulk band calculation. The average valence band edge $E_{v.av}$ relative to E_m is given by

$$E_{v.av} = E_{v.av}^i - E_m. \quad (15)$$

Next we will study the relationships between (i) the average valence band maxima $E_{v.av}^i$, $E_{v.av}$, and the average bond energy E_m , and (ii) $\text{Tr}(\varepsilon)$ and ε_{ax} , respectively. In the band calculation, the band structures of the strain are generated by the first-principles pseudopotential method. It includes scalar relativistic effects but no spin-orbit-splitting effects; the *ab initio* norm-conserving ion pseudopotentials are taken from the tables of Bachelet, Hamann, and Schluter [16, 17] and the exchange-correlation potential uses the Ceperley-Alder form [18]. The plane waves with kinetic energies up to 14.5 Ryd are included. 10 and 20 special points for the isotropic and uniaxial strains are used for sampling the k -space [19]. The method used for calculating the deformation potential is as described below (using Si as an example).

- (1) Keeping the face-centred-cubic structure unchanged for Si crystal (i.e. $a_{\perp} = a_{\parallel}$, $\varepsilon_{ax} = 0$), we select seven different lattice constant values around the Si equilibrium lattice constant (see table 1; $a_0 = 5.43 \text{ \AA}$); $\text{Tr}(\varepsilon)$ changes between -0.05 and $+0.05$. We use the band-structure calculation method to calculate the band structures for the seven different strain

states, then to calculate their average valence band maximum $E_{v.av}^i$, $E_{v.av}$, and the average bond energy E_m . For the different strain states, the calculated results for $E_{v.av}^i$, E_m , and $E_{v.av}$ are indicated by dots in figures 2(a) and 2(b). From figure 2(a), we see that the values of $E_{v.av}^i$ and E_m increase with volume compression and decrease with volume expansion. The changes of both $E_{v.av}^i$ and E_m with $\text{Tr}(\varepsilon)$ are much the same and are nearly linear. Because $E_{v.av}^i$ decreases more quickly with increase of $\text{Tr}(\varepsilon)$ than with that of E_m , $E_{v.av}$ decreases with increasing $\text{Tr}(\varepsilon)$ (see the dots in figure 2(b)). The calculated results for the change in $E_{v.av}$ with $\text{Tr}(\varepsilon)$ are obtained by linear fitting; the result is a straight line, shown in figure 2(b). Its slope $a_{v.av}$ is -0.38 eV. $a_{v.av}$ is the deformation potential corresponding to $E_{v.av}$ used to characterize quantitatively the relationship between $E_{v.av}$ and $\text{Tr}(\varepsilon)$, corresponding to a_v in the MST [2] and CNL [3] methods.

- (2) Keeping the crystal volume unchanged (i.e. $\text{Tr}(\varepsilon) = 0$), we appropriately change the value of the lattice constant a_{\parallel} on the x - y plane and the value of the lattice constant a_{\perp} on the z -axis (i.e. the uniaxially strained (001) direction), and take seven different values of ε_{ax} between -0.10 and $+0.10$. We use the band-structure calculation method to calculate the band structure for the different uniaxial strain conditions, and to find the corresponding values of $E_{v.av}^i$, E_m , and $E_{v.av}$. The calculated results are indicated by dots in figures 3(a) and 3(b). Figure 3(a) shows that $E_{v.av}^i$ and E_m are minima at $\varepsilon_{ax} = 0$. Under uniaxial strain, $E_{v.av}^i$ and E_m increase a little no matter whether ε_{ax} is larger or smaller than zero. $E_{v.av}^i$ increases a little more than E_m . Therefore, $E_{v.av}$ is minimum at $\varepsilon_{ax} = 0$. When $\varepsilon_{ax} > 0$ or $\varepsilon_{ax} < 0$, $E_{v.av}$ increases a little with increasing ε_{ax} (absolute values; see figure 3(b)). To obtain the relationship between $E_{v.av}$ and ε_{ax} , the calculated results are fitted by a quadratic expression; the fitted curve is shown in figure 3(b). Its first-order-term coefficient is zero; its quadratic-term coefficient $c_{v.av}$ is 0.91 eV. $c_{v.av}$ is also a deformation potential of second order which characterizes quantitatively the relationship between $E_{v.av}$

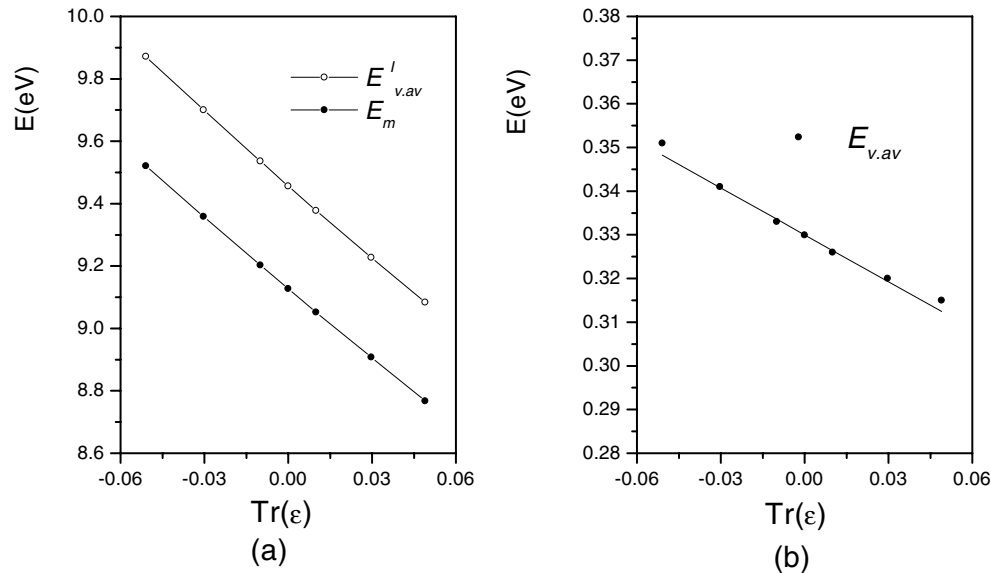


Figure 2. (a) The energy of the average valence band maxima $E_{v.av}^i$ and the average bond energy E_m as functions of the hydrostatic component $\text{Tr}(\varepsilon)$ of the strain. (b) The energy of the average valence band edge $E_{v.av}$ relative to E_m as a function of the hydrostatic component $\text{Tr}(\varepsilon)$ of the strain.

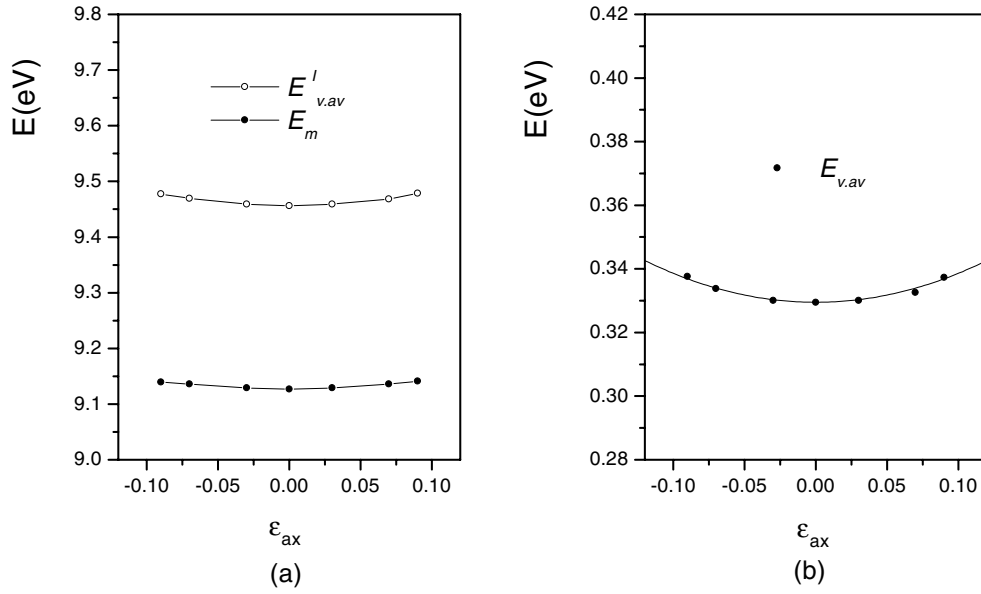


Figure 3. (a) The energy of the average valence band maxima $E_{v.av}^i$ and the average bond energy E_m as functions of the uniaxial component ϵ_{ax} of the strain. (b) The energy of the average valence band edge $E_{v.av}$ relative to E_m as a function of the uniaxial component ϵ_{ax} of the strain.

and ϵ_{ax} . At the same time, the calculated results for the value of the valence band split, δE_{001} , in seven different strain states, are linearly fitted according to equation (10) to get the shear deformation potential b of Si, and $b = -2.36$ eV.

We also use a calculation method similar to that used for Si to study the deformation potentials of Ge, InP, InAs, GaAs, AlAs, and GaP. We find that the variations are similar to that for Si. The calculated results for $a_{v.av}$, $c_{v.av}$, and b are listed in table 2. Comparing the calculated values of the deformation potential b given in table 2 with the experimental values of b given in table 1, we can see that this paper's calculated results are close to the experimental results. The $E_{v,0}$ -values in table 2 are the calculated results for the valence band maximum relative to E_m under equilibrium conditions (before deformation). For comparison, the calculated deformation potentials for the average valence band maximum, a_v , relative to the charge-neutrality level [3] and the model vacuum level [2], as well as the analogous values of the screened deformation potentials obtained by Cardona and Christensen [15], are also listed in table 2.

The strain state of the heterojunction strained layer determined by equations (6) and (7) includes volume and shape changes. In view of the above-studied results from the ABE method, we introduce two deformation potentials $a_{v.av}$ and $c_{v.av}$ to express the strain effects for the average valence band:

$$E_{v.av} = E_{v,0} + a_{v.av} \text{Tr}(\epsilon) + c_{v.av} \epsilon_{ax}^2. \quad (16)$$

Substituting equation (14) into equation (16), we get

$$E_v = E_{v,0} + a_{v.av} \text{Tr}(\epsilon) + c_{v.av} \epsilon_{ax}^2 + \Delta E_{vj,max} \quad (17)$$

where $E_{v,0}$ is the unstrained valence band edge relative to E_m , $a_{v.av} \text{Tr}(\epsilon)$ the quantum change caused by the hydrostatic strain, and $c_{v.av} \epsilon_{ax}^2$ the quantum change caused by the (001) uniaxial strain.

Table 2. The calculated results for the VBM at equilibrium, $E_{v,0}$, the calculated deformation potentials for the AVBM, $a_{v,av}$, $c_{v,av}$, relative to the ABE, and the deformation potential b obtained in this paper. The deformation potential a_v of the MST method (relative to the model vacuum level) [2] and the CNL method (relative to the charge-neutrality level) [3], and the analogous values of the screened deformation potential a_v of Cardona and Christensen (CC) [15], are also listed (in eV).

Semiconductor	This work				CNL	MST	CC
	$E_{v,0}$	$a_{v,av}$	$c_{v,av}$	b	a_v	a_v	a_v
Si	0.33	-0.38	0.91	-2.36	-2.59	2.46	-1.6
Ge	0.74	-0.31	0.52	-2.85	-4.84	1.24	-1.6
InP	-0.26	-0.15	0.31	-1.60	-2.34	1.27	-0.4
InAs	-0.03	-0.11	0.38	-1.88	-1.29	1.00	-0.6
GaP	-0.13	-0.33	0.30	-1.50		1.70	-1.5
GaAs	0.14	-0.28	0.32	-1.92	-1.68	1.16	-1.6
AlAs	-0.25	0.22	1.54	-1.67	-2.24	2.47	-1.2

In the MST [2] and CNL [3] methods, the deformation potentials of second order and likewise $c_{v,av}\varepsilon_{ax}^2$ are neglected. In order to further our understanding of the magnitude and the role of each term on the right-hand side of equation (17) and the rationality for neglecting $c_{v,av}\varepsilon_{ax}^2$, we carried out the following numerical calculation for the strained layer of the actual heterojunction under elastic strain conditions.

4. Examination of the contribution of each strain component

For the strained heterojunction, the biaxial strain tensor of the strained layer includes the hydrostatic and uniaxial components of the strain. That is, $\text{Tr}(\varepsilon)$ and ε_{ax} are not equal to zero; the effect of both of them on E_v should be considered (equation (17)). For simplicity, the notation for the strained heterojunction is as follows: the material above the backwards oblique line ‘\’ or forwards oblique line ‘/’ is the strained layer, while that below it is the substrate. That is, A/B means that B is used as the substrate, and A is the strained layer, while A\B means that A is used as the substrate, and B is the strained layer. Table 3 includes 14 kinds

Table 3. The calculated results for $a_{v,av}$, $\text{Tr}(\varepsilon)$, $c_{v,av}\varepsilon_{ax}^2$, and $\Delta E_{vj,max}$ (in eV).

Strained layer	Substrate	a_{\parallel}^B	$\text{Tr}(\varepsilon)$	ε_{ax}	$a_{v,av}$	$\text{Tr}(\varepsilon)$	$c_{v,av}\varepsilon_{ax}^2$	$\Delta E_{vj,max}$
Ge	Si	5.43	-0.0486	0.0682	0.015	0.002	0.295	
Si	Ge	5.65	0.0496	-0.0720	-0.019	0.005	0.303	
InAs	GaAs	5.65	-0.0617	0.1412	0.007	0.008	0.381	
GaAs	InAs	6.06	0.0774	-0.1403	-0.022	0.006	0.507	
InAs	AlAs	5.65	-0.0617	0.1412	0.007	0.008	0.381	
AlAs	InAs	6.06	0.0831	-0.1346	0.018	0.028	0.428	
InP	GaAs	5.65	-0.0327	0.0797	0.005	0.002	0.164	
GaAs	InP	5.87	0.0415	-0.0753	-0.012	0.002	0.303	
InP	InAs	6.06	0.0283	-0.0689	-0.004	0.001	0.228	
InAs	InP	5.87	-0.0286	0.0655	0.003	0.002	0.244	
GaP	GaAs	5.65	0.0408	-0.0693	-0.013	0.001	0.212	
GaAs	GaP	5.45	-0.0377	0.0685	0.011	0.001	0.230	
InP	GaP	5.45	-0.0624	0.1522	0.009	0.007	0.280	
GaP	InP	5.87	0.0857	-0.1454	-0.028	0.006	0.438	

of strained heterojunction. They are Si\Ge, Si/Ge, GaAs\InAs, GaAs/InAs, AlAs\InAs, AlAs/InAs, GaAs\InP, GaAs/InP, InP\InAs, InP/InAs, GaP\GaAs, GaP/GaAs, GaP\InP, and GaP/InP. The values of a_{\parallel} for the strained layers are the same as the equilibrium lattice constants of the substrates. From the lattice constants and the elastic coefficients given in table 1, a_{\perp} for the strained layer is calculated from equations (6) and (7), and $\text{Tr}(\varepsilon)$ and ε_{ax} are calculated from equations (8) and (9). Then $a_{v,av} \text{Tr}(\varepsilon)$ and $c_{v,av} \varepsilon_{ax}^2$ are determined from the calculated results for the deformations $a_{v,av}$ and $c_{v,av}$ listed in table 2. At the same time, $\Delta E_{vj,max}$ can be determined using the experimental values of b and Δ_0 given in table 1 through equations (11)–(13). All of the calculated results are listed in table 3.

From table 3, for the three strain-effect terms in equation (17), $a_{v,av} \text{Tr}(\varepsilon)$, $c_{v,av} \varepsilon_{ax}^2$, and $\Delta E_{vj,max}$, the value of $c_{v,av} \varepsilon_{ax}^2$ is a minimum, and can be neglected; the value of $\Delta E_{vj,max}$ is at its largest and is the main factor determining the E_v -value; the value of $a_{v,av} \text{Tr}(\varepsilon)$ is somewhat larger than that of $c_{v,av} \varepsilon_{ax}^2$. Neglecting $c_{v,av} \varepsilon_{ax}^2$ in equation (17), the expression for E_v is simplified to

$$E_v = E_{v,0} + a_{v,av} \text{Tr}(\varepsilon) + \Delta E_{vj,max}. \quad (18)$$

The value of $E_{v,0}$ in table 2 and the value of $\Delta E_{vj,max}$ in table 3 are of the same order of magnitude. Therefore both of them are major factors in determining the E_v -value. But the value of $a_{v,av} \text{Tr}(\varepsilon)$ is much smaller than both of them. Since the absolute value of $a_{v,av}$ in the ABE method is much smaller than the absolute value of a_v in the MST [2] and CNL [3] methods (see table 2), the absolute value of $a_{v,av} \text{Tr}(\varepsilon)$ is especially small. This is an important feature of the ABE method. Next, we study further the effect of $a_{v,av} \text{Tr}(\varepsilon)$ on E_v and the VBO.

5. Simplification of the ABE method and results of the application to strain

From table 2, it can be seen that the value of $a_{v,av}$ in this paper is about an order of magnitude smaller than the value of a_v in the CNL [3] method, and is even much smaller than the value of a_v in the MST [2] method in absolute value. Therefore, for the ABE method, it is necessary to understand further the effect of the $a_{v,av} \text{Tr}(\varepsilon)$ term on ΔE_v for the strained heterojunction. In the calculation of E_v and ΔE_v , if we retain the $a_{v,av} \text{Tr}(\varepsilon)$ term in equation (18) (this is called method 1), or neglect the $a_{v,av} \text{Tr}(\varepsilon)$ term (this is called method 2), the values of $E_{v,0}$, $a_{v,av} \text{Tr}(\varepsilon)$, and $\Delta E_{vj,max}$ are taken from tables 2 and 3. For the calculation of E_v for the substrate material (unstrained), since the calculated band structures do not include the spin-orbit effect, $E_v = E_{v,0} - \frac{1}{3} \Delta_0$ was added to E_v *a posteriori*—where the values of $E_{v,0}$ and Δ_0 are taken from table 2 and table 1, respectively. Using the calculated results for the strained layer and the substrate, ΔE_v for the strained heterojunction can be obtained from equation (5). The results calculated by method 1 and method 2 are listed in table 4 for 14 kinds of heterojunction. The results from the CNL [3] and MST [2] methods and the experiments are also listed for comparison.

From the results in table 4, we can obtain the following conclusions:

- (1) For nine kinds of strained heterojunction for which the experimental values of ΔE_v have been found, the extent of the agreement of the results calculated in this paper with the experimental data is better than for the MST and CNL methods for GaAs\InAs, GaAs/InAs, AlAs\InAs, AlAs/InAs, Si/Ge, and GaP\GaAs heterojunctions; it is only worse than for the MST and CNL methods for GaAs\InP and GaAs/InP heterojunctions.
- (2) From the results calculated by method 1 and method 2 and given in table 4, we can see that the change of ΔE_v is less than 0.03 eV, which is within experimental error. Therefore,

Table 4. Calculated valence band offsets ΔE_v of A/B and A\B. The results from the MST [2] and CNL [3] methods and from experiment are also listed for comparison. A positive valence band offset means that the valence band edge of semiconductor A (Sm.A) lies at a lower position than that of semiconductor B. The experimental values are quoted from reference [3] except where otherwise indicated.

A/B or A\B	$a_{ }$	Sm.A	ΔE_v				
			Method 1	Method 2	CNL	MST	Experiment
Si\Ge	5.43	Si	0.71	0.69	0.61	0.88	0.74 and 0.83
Si/Ge	5.65	Si	0.23	0.21	0.00	0.32	0.17 and 0.22
GaAs\InAs	5.65	GaAs	0.10	0.10	0.32	0.43	-0.04 and 0.17 ^a
GaAs/InAs	6.06	GaAs	-0.53	-0.55	-0.33	-0.30	-0.52
AlAs\InAs	5.65	AlAs	0.51	0.51	0.70	1.02	0.29 and 0.5 ^b
AlAs/InAs	6.06	AlAs	-0.10	-0.08	0.23	0.29	-0.10
GaAs\InP	5.65	GaAs	-0.34	-0.35	-0.25	-0.11	-0.17
GaAs/InP	5.87	GaAs	-0.65	-0.67	-0.60	-0.46	-0.56
InP\InAs	5.87	InP	0.44	0.44		0.54	
InP/InAs	6.06	InP	0.13	0.13		0.21	
GaP\GaAs	5.45	GaP	0.48	0.47		0.66	0.55 ^c and 0.43 ^d
GaP/GaAs	5.65	GaP	0.18	0.17		0.28	
GaP\InP	5.45	GaP	0.13	0.12		0.22	
GaP/InP	5.87	GaP	-0.50	-0.53		-0.54	

^a Reference [20].

^b Reference [21].

^c Reference [22].

^d Reference [23].

for the calculation of ΔE_v based on the average-bond-energy method, the formula for calculating E_v (equation (18)) can be further simplified to

$$E_v = E_{v,0} + \Delta E_{vj,max}. \quad (19)$$

Thus, it is clear that the value of ΔE_v for the strained heterojunction can be obtained by a simple algebraic operation if $E_{v,0}$ for the unstrained bulk material and the experimental values of b and Δ_0 are known (see equations (11)–(13)). There is no need to calculate the strained band structures and deformation potentials $a_{v,av}$. Obviously, this will considerably reduce the calculational burden and make it equivalent to that for a normal lattice-matched heterojunction. This is a unique advantage of the ABE method. Because in the MST [2] and CNL [3] methods, the value of a_v (absolute value) is not small enough (see table 2), a similar simplification cannot be made. Thus, for the VBO calculation for a strained heterojunction based on the ABE method, the calculational burden will be smaller than those in the MST [2] and CNL [3] methods.

- (3) The simplified scheme for calculation of the strained-heterojunction VBO by the ABE method (refer to equations (19) and (5)) provides a more definite physical picture. That is, the strained-heterojunction VBO consists of two parts: one is the difference between the positions of the valence band maxima of the two bulk materials at equilibrium (i.e. unstrained; the difference is $E_{v,0}(B) - E_{v,0}(A)$); the other is the change of the valence band edge caused by the interaction between the shear strains and with the spin-orbit splitting, $\Delta E_{vj,max}$. The latter can be adjusted by changing the strain state. Therefore, provided that we know the experimental values of the lattice constants, elastic coefficients, spin-orbit splitting energies Δ_0 , and shear deformation potentials b for the

two semiconductors which constitute the heterojunction, the valence band offset of the strained heterojunction can be predicted.

- (4) The valence band edge $E_{v,av}$ is, relative to the reference level, $E_{v,av} = E_{v,av}^i - E_r$, where the average valence band maximum $E_{v,av}^i$ is given by a band calculation, and E_r designates the reference level. Due to the different reference levels, the deformation potentials a_v of the CNL and MST methods are different, and their signs are opposite. For the MST and ABE methods, the deformation potentials corresponding to $E_{v,av}$, $E_{v,av}^i$, and E_r can be represented as $a_v = a_i - a_r$ and $a_{v,av} = a_i - a_m$; both $E_{v,av}^i$ are generated by *ab initio* pseudopotential band calculations for the semiconductor crystal changing with strain. Because both of the values of $E_{v,av}^i$ as functions of $\text{Tr}(\varepsilon)$ are the same, the values of a_i will be the same too. The difference between a_v and $a_{v,av}$ arises mainly from the difference of the deformation potentials from the reference level. It is an intrinsic property of the average bond energy that the value of $a_{v,av}$ is extremely small. Therefore, the simplified calculation scheme for the strained-heterojunction VBO just relies on a characteristic of the ABE method.

6. Conclusions

The procedure of the ABE method for calculating the strained-heterojunction VBO is analogous to the procedures of the MST [2] and CNL [3] methods. We use the position of the average band edge $E_{v,av}$ relative to the average bond energy, instead of $E_{v,av}$ as used in the MST and CNL methods, which is calculated relative to the model vacuum level and the charge-neutrality level, respectively. The calculated deformation potentials $a_{v,av}$ corresponding to $E_{v,av}$ are quite different from the equivalent a_v of the MST and CNL methods. Note that all deformation potentials a_v of the CNL method have opposite sign to those of the MST method. We also show that the magnitude of the deformation potentials a_v is determined by an intrinsic property of the reference level. Any reference-level theory regarding band offsets can be extended to the case of strain by a similar procedure; however, the deformation potentials $a_{v,av}$ of the ABE method are particularly small and negligible. Thus it is only necessary to calculate the valence band edge $E_{v,0}$ relative to the average bond energy for zero strain, and to use the experimental values of b and Δ_0 to calculate the value of the VBO of the strained heterojunction. It is not necessary to calculate the band structures of the different strain states, and this will be convenient in predicting band offsets of strained heterojunctions.

Acknowledgments

This work was supported by the Colleges and Universities Doctors Fund (9538409) and Fujian Natural Science Fund (E9910005).

References

- [1] Van de Walle C G and Martin R M 1987 *Phys. Rev. B* **35** 8154
- [2] Van de Walle C G 1989 *Phys. Rev. B* **39** 1871
- [3] Ohler C, Daniels C, Förstr A and Lüth H 1998 *Phys. Rev. B* **58** 7864
- [4] Tersoff J 1984 *Phys. Rev. Lett.* **52** 465
- [5] Wang R Z, Ke S H and Huang M C 1992 *J. Phys.: Condens. Matter* **4** 8083
- [6] Christensen N E 1988 *Phys. Rev. B* **37** 4528
- [7] Wei S H and Zunger A 1998 *Appl. Phys. Lett.* **72** 2011
- [8] Cardona M and Christensen N E 1988 *Phys. Rev. B* **35** 6182
- [9] Flores F and Tejedor C 1979 *J. Phys. C: Solid State Phys.* **12** 731

- [10] Harrison W A and Tersoff J 1986 *J. Vac. Sci. Technol. B* **4** 1068
- [11] Chen A B and Sher A 1981 *Phys. Rev. B* **23** 5360
- [12] Wang R Z, Ke S H and Huang M C 1995 *Phys. Rev. B* **51** 1935
- [13] Ke S H, Wang R Z and Huang M C 1997 *Z. Phys. B* **102** 61
- [14] Binberg D *et al* 1982 *Landolt-Börnstein New Series Group III*, vol 17, Part A, ed O Madelung (Berlin: Springer)
- [15] Cardona M and Christensen N E 1987 *Phys. Rev. B* **35** 6182
- [16] Hamann D R, Schluter M and Chiang C 1979 *Phys. Rev. Lett.* **43** 1494
- [17] Bachelet G B, Hamann D R and Schluter M 1982 *Phys. Rev. B* **26** 4199
- [18] Ceperley D and Alder B J 1980 *Phys. Rev. Lett.* **45** 566
- [19] Chadi D J and Cohen M L 1973 *Phys. Rev. B* **8** 5747
- [20] Kowalczyk S P, Schaffer W J, Kraut E A and Grant R W 1982 *J. Vac. Sci. Technol.* **20** 705
- [21] Arriaga J *et al* 1991 *Phys. Rev. B* **43** 2050
- [22] Katnani A D and Margaritondo G 1983 *Phys. Rev. B* **28** 1944
- [23] Recio M, Armelles G, Melendea J and Briones F 1990 *J. Appl. Phys.* **67** 2044